

Supplementary Information for “Atomic configuration controlled photocurrent in van der Waals homostructures”

Contents of the Supplementary Information

I. Symmetry and Stacking Analysis of Shift Vector in van der Waals materials and homostructures

- A. *Shift Vector Configuration Dependence for Bernal Stacked BLG*
- B. *Shift Vector Configuration Dependence for Staggered Sublattice Potential, e.g. G/hBN*
- C. *Shift Vector Configuration Dependence for Monolayer TMDs*
- D. *Shift Vector Configuration Dependence for 2H Stacked Bilayer TMDs*

II. Strained shift current induced by unpolarized light

III. Hamiltonian of Bernal Stacked BLG

IV. Numerical Calculation of Shift Vector in AB stacked BLG for other polarizations

I. Symmetry and Stacking Analysis of Shift Vector in van der Waals materials and homostructures

In this section, we present the shift vector dependence on the symmetry and stacking arrangement in van der Waals (vdW) materials and homostructures. We show that the shift vector is highly sensitive to the local atomic configuration of the structure, leading to stacking and polarisation dependent SPC. In general, the real space shift of photo-excited electrons can be described by a shift vector $\mathbf{r}(\theta, \mathbf{k})^{1,2}$ as displayed in Eq. (1) of the main text:

$$\mathbf{r}(\theta, \mathbf{k}) = \mathbf{A}_c(\mathbf{k}) - \mathbf{A}_v(\mathbf{k}) - \nabla_{\mathbf{k}} \arg[\nu_{\theta}(\mathbf{k})]. \quad (\text{S1})$$

For our symmetry and stacking analysis below, it will be useful to re-express this conventional form of the shift vector in terms of a Wilson line^{3,4}:

$$\mathbf{r}(\theta, \mathbf{k}) = \lim_{\mathbf{q} \rightarrow 0} \nabla_{\mathbf{q}} \arg[\mathcal{W}(\theta, \mathbf{k}, \mathbf{q})], \quad (\text{S2})$$

where θ is the electric field polarisation angle of the incident light with respect to the x , \mathbf{k} is the wavevector measured from the Γ point, and

$$\mathcal{W}(\theta, \mathbf{k}, \mathbf{q}) = \langle u_v(\mathbf{k}) | u_v(\mathbf{k} + \mathbf{q}) \rangle \langle u_v(\mathbf{k} + \mathbf{q}) | \nu_{\theta} | u_c(\mathbf{k} + \mathbf{q}) \rangle \langle u_c(\mathbf{k} + \mathbf{q}) | u_c(\mathbf{k}) \rangle. \quad (\text{S3})$$

Here $|u_{c(v)}(\mathbf{k})\rangle$ is the Bloch wavefunction of the conduction (valence) band. The velocity matrix $\nu_{\theta} = \hat{v} \cdot \hat{\mathbf{e}}_{\theta}$ is a function of the polarisation direction $\hat{\mathbf{e}}_{\theta}$. For linearly polarised light, we have $\nu_{\theta} = \nu_x \cos \theta + \nu_y \sin \theta$. We note that though the Wilson line $\mathcal{W}(\theta, \mathbf{k}, \mathbf{q})$ depends on the gauge choice of the wavefunction, the gradient of its phase $\nabla_{\mathbf{q}} \arg[\mathcal{W}(\theta, \mathbf{k}, \mathbf{q})]$ and the shift vector are gauge invariant. In the following, we examine the properties of $\langle u_n(\mathbf{k}) | u_m(\mathbf{q}) \rangle$ and $\langle u_n(\mathbf{k}) | \nu_{\theta} | u_m(\mathbf{q}) \rangle$ in different vdW materials and homostructures and the atomic configuration dependence of the shift vector and SPC. In particular, we illustrate the configuration dependent SPC in Bernal stacked bilayer graphene (BLG), graphene on hexagonal boron nitride (G/hBN), monolayer transition metal dicalcogenide (TMD) and 2H stacked bilayer TMD.

A. Shift Vector Configuration Dependence for Bernal Stacked BLG

Bernal stacked BLG possesses a three-fold rotational symmetry C_3^z and mirror symmetry about the armchair direction, as shown in Fig. 1 in the main text (e.g., the y -axis in Fig. 1). Applying an interlayer electric potential difference Δ breaks the inversion symmetry of the system. As we see below, this gives rise to a nonzero SPC.

Two stacking configurations are possible in Bernal stacked BLG: AB stacking whereby the A site of the top layer is directly on top of the B site of the bottom layer and BA stacking whereby the B site of the top layer is directly

on top of the A site of the bottom layer. Here we describe AB/BA stacked BLG with the real space Hamiltonian $\mathcal{H}^{(\eta)}(\Delta, \mathbf{r})$, where $\eta = \text{AB, BA}$ denotes the stacking configuration and Δ denotes the interlayer potential difference. In the following, we examine the symmetry constraints of the shift vector $\mathbf{r}^{(\eta)}(\Delta, \theta, \mathbf{k})$ and the stacking and configuration dependence of the SPC.

1. Time Reversal Symmetry

BLG exhibits spin degeneracy and can be considered an effectively spinless system. In the presence of time reversal symmetry \mathcal{T} , the Bloch Hamiltonian $H^{(\eta)}(\Delta, \mathbf{k}) = e^{-i\mathbf{k}\cdot\mathbf{r}}\mathcal{H}^{(\eta)}(\Delta, \mathbf{r})e^{i\mathbf{k}\cdot\mathbf{r}}$ satisfies $\mathcal{T}H^{(\eta)}(\Delta, \mathbf{k})\mathcal{T}^{-1} = H^{(\eta)}(\Delta, -\mathbf{k})$. The Bloch wavefunction of band n , $|u_n^{(\eta)}(\Delta, \mathbf{k})\rangle$ is defined such that $H^{(\eta)}(\Delta, \mathbf{k})|u_n^{(\eta)}(\Delta, \mathbf{k})\rangle = \epsilon_n^{(\eta)}(\Delta, \mathbf{k})|u_n^{(\eta)}(\Delta, \mathbf{k})\rangle$, where $\epsilon_n^{(\eta)}(\Delta, \mathbf{k})$ is the energy eigenvalue of band n . By considering $\mathcal{T}H^{(\eta)}(\Delta, \mathbf{k})|u_n^{(\eta)}(\Delta, \mathbf{k})\rangle$, we find that the Bloch wavefunction transforms as:

$$\epsilon_n^{(\eta)}(\Delta, \mathbf{k}) = \epsilon_n^{(\eta)}(\Delta, -\mathbf{k}), \quad \mathcal{T}|u_n^{(\eta)}(\Delta, \mathbf{k})\rangle = |u_n^{(\eta)}(\Delta, -\mathbf{k})\rangle^*. \quad (\text{S4})$$

Thus, for any wavevectors \mathbf{k}_1 and \mathbf{k}_2 measured from the centre of the Brillouin zone, we have

$$\langle u_m^{(\eta)}(\Delta, \mathbf{k}_1)|u_n^{(\eta)}(\Delta, \mathbf{k}_2)\rangle = \langle u_m^{(\eta)}(\Delta, \mathbf{k}_1)|\mathcal{T}^{-1}\mathcal{T}|u_n^{(\eta)}(\Delta, \mathbf{k}_2)\rangle = \langle u_m^{(\eta)}(\Delta, -\mathbf{k}_1)|u_n^{(\eta)}(\Delta, -\mathbf{k}_2)\rangle^*. \quad (\text{S5})$$

The velocity operator is odd under time reversal: $\mathcal{T}\hat{v}^{(\eta)}(\Delta)\mathcal{T}^{-1} = -\hat{v}^{(\eta)}(\Delta)$. Thus, the velocity matrix element satisfies

$$\begin{aligned} \langle u_m^{(\eta)}(\Delta, \mathbf{k}_1)|\nu_\theta^{(\eta)}(\Delta)|u_n^{(\eta)}(\Delta, \mathbf{k}_2)\rangle &= \langle u_m^{(\eta)}(\Delta, \mathbf{k}_1)|\mathcal{T}^{-1}\mathcal{T}\nu_\theta^{(\eta)}(\Delta)\mathcal{T}^{-1}|u_n^{(\eta)}(\Delta, \mathbf{k}_2)\rangle \\ &= -\langle u_m^{(\eta)}(\Delta, -\mathbf{k}_1)|\nu_\theta^{(\eta)}(\Delta)|u_n^{(\eta)}(\Delta, -\mathbf{k}_2)\rangle^*. \end{aligned} \quad (\text{S6})$$

Similarly, we obtain the symmetry constraint for the Wilson line:

$$\mathcal{W}^{(\eta)}(\Delta, \theta, \mathbf{k}, \mathbf{q}) = -[\mathcal{W}^{(\eta)}(\Delta, \theta, -\mathbf{k}, -\mathbf{q})]^*, \quad \arg[\mathcal{W}^{(\eta)}(\Delta, \theta, \mathbf{k}, \mathbf{q})] = -\arg[\mathcal{W}^{(\eta)}(\Delta, \theta, -\mathbf{k}, -\mathbf{q})] + \pi. \quad (\text{S7})$$

As a result, the shift vector in a time-reversal invariant system is even in k -space:

$$\mathbf{r}^{(\eta)}(\Delta, \theta, \mathbf{k}) = \mathbf{r}^{(\eta)}(\Delta, \theta, -\mathbf{k}). \quad (\text{S8})$$

2. Inversion Operation and Interlayer Potential Dependence

In AB/BA stacked bilayer BLG, the interlayer potential difference Δ breaks the inversion symmetry. Here we show that breaking of the inversion symmetry is necessary to induce a finite SPC. Furthermore, switching the direction of the interlayer potential flips the sign of the shift vector – as a result, SPC flows in the opposite direction.

To see this, we observe that upon spatial inversion, the atomic configuration of the BLG remains unchanged but the interlayer potential difference Δ flips sign. The real-space Hamiltonian satisfies $\mathcal{I}\mathcal{H}^{(\eta)}(\Delta, \mathbf{r})\mathcal{I}^{-1} = \mathcal{H}^{(\eta)}(\Delta, -\mathbf{r}) = \mathcal{H}^{(\eta)}(-\Delta, \mathbf{r})$. Thus, under inversion, the Bloch Hamiltonian transforms as $\mathcal{I}H^{(\eta)}(\Delta, \mathbf{k})\mathcal{I}^{-1} = H^{(\eta)}(-\Delta, -\mathbf{k})$. By considering $\mathcal{I}H^{(\eta)}(\mathbf{k})|u_n^{(\eta)}(\mathbf{k})\rangle$, one arrives at

$$\epsilon_n^{(\eta)}(\Delta, \mathbf{k}) = \epsilon_n^{(\eta)}(-\Delta, -\mathbf{k}), \quad \mathcal{I}|u_n^{(\eta)}(\Delta, \mathbf{k})\rangle = |u_n^{(\eta)}(-\Delta, -\mathbf{k})\rangle \quad (\text{S9})$$

This gives

$$\langle u_m^{(\eta)}(\Delta, \mathbf{k}_1)|u_n^{(\eta)}(\Delta, \mathbf{k}_2)\rangle = \langle u_m^{(\eta)}(\Delta, \mathbf{k}_1)|\mathcal{I}^{-1}\mathcal{I}|u_n^{(\eta)}(\Delta, \mathbf{k}_2)\rangle = \langle u_m^{(\eta)}(-\Delta, -\mathbf{k}_1)|u_n^{(\eta)}(-\Delta, -\mathbf{k}_2)\rangle. \quad (\text{S10})$$

Upon inversion, velocity operator transforms as $\mathcal{I}\hat{v}^{(\eta)}(\Delta)\mathcal{I}^{-1} = -\hat{v}^{(\eta)}(-\Delta)$. Thus for electric field polarisation θ , we have

$$\begin{aligned} \langle u_m^{(\eta)}(\Delta, \mathbf{k}_1)|\nu_\theta^{(\eta)}(\Delta)|u_n^{(\eta)}(\Delta, \mathbf{k}_2)\rangle &= \langle u_m^{(\eta)}(\Delta, \mathbf{k}_1)|\mathcal{I}^{-1}\mathcal{I}\nu_\theta^{(\eta)}(\Delta)\mathcal{I}^{-1}|u_n^{(\eta)}(\Delta, \mathbf{k}_2)\rangle \\ &= -\langle u_m^{(\eta)}(-\Delta, -\mathbf{k}_1)|\nu_\theta^{(\eta)}(-\Delta)|u_n^{(\eta)}(-\Delta, -\mathbf{k}_2)\rangle. \end{aligned} \quad (\text{S11})$$

Using these relations above, the Wilson line satisfies

$$\mathcal{W}^{(\eta)}(\Delta, \theta, \mathbf{k}, \mathbf{q}) = -\mathcal{W}^{(\eta)}(-\Delta, \theta, -\mathbf{k}, -\mathbf{q}), \quad \arg[\mathcal{W}^{(\eta)}(\Delta, \theta, \mathbf{k}, \mathbf{q})] = \arg[\mathcal{W}^{(\eta)}(-\Delta, \theta, -\mathbf{k}, -\mathbf{q})] + \pi, \quad (\text{S12})$$

and the shift vector satisfies

$$\mathbf{r}^{(\eta)}(\Delta, \theta, \mathbf{k}) = -\mathbf{r}^{(\eta)}(-\Delta, \theta, -\mathbf{k}). \quad (\text{S13})$$

Importantly, when $\Delta = 0$, the above relation demands that the shift vector is odd in the k -space. Since $\rho^{(\eta)}(\Delta, \mathbf{k})$ and $|\nu_\theta^{(\eta)}(\Delta)|^2$ are both even, upon integrating the weighted shift vector in the Brillouin zone [see Eq. (2) of the main text], we obtain the well-known vanishing of SPC in an inversion symmetric system. Thus, inversion symmetry has to be broken to obtain finite SPC.

We note that by further applying time reversal symmetry (see above section) where $\mathbf{r}^{(\eta)}$ is even in the k -space [Eq. (S8)], we arrive at the dependence of shift vector on the sign of interlayer potential:

$$\mathbf{r}^{(\eta)}(\Delta, \theta, \mathbf{k}) = -\mathbf{r}^{(\eta)}(-\Delta, \theta, \mathbf{k}). \quad (\text{S14})$$

The shift vector switches sign when the interlayer potential difference is reversed. We see in Fig. 1b in the main text that this is manifested in opposite SPC for $\Delta \rightarrow -\Delta$.

3. Mirror Symmetry

Bernal stacked BLG exhibits mirror symmetry about the armchair directions. In the coordinate system shown in Fig. 1 in the main text, one of the mirror reflection axis is along the y direction; the system is invariant under the mirror operation $\mathcal{M}_y : (x, y, z) \rightarrow (-x, y, z)$. The real space Hamiltonian obeys $\mathcal{M}_y \mathcal{H}^{(\eta)}(\Delta, \mathbf{r}) \mathcal{M}_y^{-1} = \mathcal{H}^{(\eta)}(\Delta, \mathbf{r})$. The Bloch Hamiltonian thus satisfies $\mathcal{M}_y H^{(\eta)}(\Delta, \mathbf{k}) \mathcal{M}_y^{-1} = H^{(\eta)}(\Delta, \mathcal{M}_y \mathbf{k})$ and we have

$$\epsilon_n^{(\eta)}(\Delta, \mathbf{k}) = \epsilon_n^{(\eta)}(\Delta, \mathcal{M}_y \mathbf{k}), \quad \mathcal{M}_y |u_n^{(\eta)}(\Delta, \mathbf{k})\rangle = |u_n^{(\eta)}(\Delta, \mathcal{M}_y \mathbf{k})\rangle. \quad (\text{S15})$$

The above relation gives

$$\langle u_m^{(\eta)}(\Delta, \mathbf{k}_1) | u_n^{(\eta)}(\Delta, \mathbf{k}_2) \rangle = \langle u_m^{(\eta)}(\Delta, \mathbf{k}_1) | \mathcal{M}_y^{-1} \mathcal{M}_y | u_n^{(\eta)}(\Delta, \mathbf{k}_2) \rangle = \langle u_m^{(\eta)}(\Delta, \mathcal{M}_y \mathbf{k}_1) | u_n^{(\eta)}(\Delta, \mathcal{M}_y \mathbf{k}_2) \rangle. \quad (\text{S16})$$

Under \mathcal{M}_y , the x component of the velocity operator switches sign $\mathcal{M}_y \nu_x^{(\eta)}(\Delta) \mathcal{M}_y^{-1} = -\nu_x^{(\eta)}(\Delta)$ while the y component remains invariant $\mathcal{M}_y \nu_y^{(\eta)}(\Delta) \mathcal{M}_y^{-1} = \nu_y^{(\eta)}(\Delta)$, thus we have $\mathcal{M}_y \nu_\theta^{(\eta)}(\Delta) \mathcal{M}_y^{-1} = \nu_{\pi-\theta}^{(\eta)}(\Delta)$. This gives

$$\begin{aligned} \langle u_m^{(\eta)}(\Delta, \mathbf{k}_1) | \nu_\theta^{(\eta)}(\Delta) | u_n^{(\eta)}(\Delta, \mathbf{k}_2) \rangle &= \langle u_m^{(\eta)}(\Delta, \mathbf{k}_1) | \mathcal{M}_y^{-1} \mathcal{M}_y \nu_\theta^{(\eta)}(\Delta) \mathcal{M}_y^{-1} \mathcal{M}_y | u_n^{(\eta)}(\Delta, \mathbf{k}_2) \rangle \\ &= \langle u_m^{(\eta)}(\Delta, \mathcal{M}_y \mathbf{k}_1) | \nu_{\pi-\theta}^{(\eta)}(\Delta) | u_n^{(\eta)}(\Delta, \mathcal{M}_y \mathbf{k}_2) \rangle. \end{aligned} \quad (\text{S17})$$

Using these relations above, the Wilson line satisfies

$$\mathcal{W}^{(\eta)}(\Delta, \theta, \mathbf{k}, \mathbf{q}) = \mathcal{W}^{(\eta)}(\Delta, \pi - \theta, \mathcal{M}_y \mathbf{k}, \mathcal{M}_y \mathbf{q}), \quad \arg[\mathcal{W}^{(\eta)}(\Delta, \theta, \mathbf{k}, \mathbf{q})] = \arg[\mathcal{W}^{(\eta)}(\Delta, \pi - \theta, \mathcal{M}_y \mathbf{k}, \mathcal{M}_y \mathbf{q})], \quad (\text{S18})$$

and shift vector thus satisfies

$$r_x^{(\eta)}(\Delta, \theta, \mathbf{k}) = -r_x^{(\eta)}(\Delta, \pi - \theta, \mathcal{M}_y \mathbf{k}), \quad r_y^{(\eta)}(\Delta, \theta, \mathbf{k}) = r_y^{(\eta)}(\Delta, \pi - \theta, \mathcal{M}_y \mathbf{k}). \quad (\text{S19})$$

We note, parenthetically, for a given ac electric field (light irradiation), the polarisations along $\hat{\mathbf{e}}$ and $-\hat{\mathbf{e}}$ directions are equivalent and yield the same shift vector. To see this, we observe that $\nu_\theta^{(\eta)}(\Delta) = -\nu_{\theta+\pi}^{(\eta)}(\Delta)$ and

$$\mathcal{W}^{(\eta)}(\Delta, \theta, \mathbf{k}, \mathbf{q}) = -\mathcal{W}^{(\eta)}(\Delta, \theta + \pi, \mathbf{k}, \mathbf{q}), \quad \arg[\mathcal{W}^{(\eta)}(\Delta, \theta, \mathbf{k}, \mathbf{q})] = \arg[\mathcal{W}^{(\eta)}(\Delta, \theta + \pi, \mathbf{k}, \mathbf{q})] + \pi. \quad (\text{S20})$$

Since the shift vector is the gradient of the argument of the Wilson line, an additional π phase shift for $\mathcal{W}^{(\eta)}(\Delta, \theta, \mathbf{k}, \mathbf{q})$ does not affect the shift vector

$$\mathbf{r}^{(\eta)}(\Delta, \theta, \mathbf{k}) = \mathbf{r}^{(\eta)}(\Delta, \theta + \pi, \mathbf{k}). \quad (\text{S21})$$

Thus, Eq. (S19) can be rewritten as

$$r_x^{(\eta)}(\Delta, \theta, \mathbf{k}) = -r_x^{(\eta)}(\Delta, -\theta, \mathcal{M}_y \mathbf{k}), \quad r_y^{(\eta)}(\Delta, \theta, \mathbf{k}) = r_y^{(\eta)}(\Delta, -\theta, \mathcal{M}_y \mathbf{k}). \quad (\text{S22})$$

Furthermore, combining Eq. (S8) and (S22), the composition of time reversal \mathcal{T} and mirror symmetry \mathcal{M}_y yields

$$r_x^{(\eta)}(\Delta, \theta, \mathbf{k}) = -r_x^{(\eta)}(\Delta, -\theta, k_x, -k_y), \quad r_y^{(\eta)}(\Delta, \theta, \mathbf{k}) = r_y^{(\eta)}(\Delta, -\theta, k_x, -k_y). \quad (\text{S23})$$

Eq. (S23) gives the symmetry constraints for the shift vector, which is manifested as the constraints for the direction of the SPC when the electric field is polarised along high-symmetry axes. For example, when the electric field polarisation is normal to the mirror plane (i.e. $\theta = 0, \pi$), the shift vector satisfies

$$r_x^{(\eta)}(\Delta, 0, \mathbf{k}) = -r_x^{(\eta)}(\Delta, 0, k_x, -k_y), \quad r_y^{(\eta)}(\Delta, 0, \mathbf{k}) = r_y^{(\eta)}(\Delta, 0, k_x, -k_y). \quad (\text{S24})$$

Since both $\rho(\mathbf{k})$ and $|\nu_\theta^{(\eta)}(\Delta)|^2$ are even under $k_y \rightarrow -k_y$, the symmetry constraint in Eq. (S24) ensures that upon integration in the k -space [Eq. (2) in the main text], the x component of the SPC vanishes while the y component is nonzero. Thus, for linear polarisation normal to the mirror plane, SPC is completely transverse.

Similarly, when the electric field is polarised along the mirror reflection axis (i.e. $\theta = \pm\pi/2$), Eq. (S23) reduces to

$$r_x^{(\eta)}(\Delta, \pi/2, \mathbf{k}) = -r_x^{(\eta)}(\Delta, \pi/2, k_x, -k_y), \quad r_y^{(\eta)}(\Delta, \pi/2, \mathbf{k}) = r_y^{(\eta)}(\Delta, \pi/2, k_x, -k_y). \quad (\text{S25})$$

Since $r_x^{(\eta)}(\Delta, \pi/2, \mathbf{k})$ is odd in k_y while $r_y^{(\eta)}(\Delta, \pi/2, \mathbf{k})$ is even, Eq. (S25) implies that SPC is along the y direction. Thus, for electric field polarisation parallel to the mirror plane, we obtain completely longitudinal SPC.

4. In-plane Three-fold Rotational Symmetry

The BLG lattice is invariant under in-plane three-fold rotational symmetry C_3^z such that $C_3^z \mathcal{H}^{(\eta)}(\Delta, \mathbf{r})(C_3^z)^{-1} = \mathcal{H}^{(\eta)}(\Delta, \mathbf{r})$. The Bloch Hamiltonian thus obeys the relation $C_3^z H^{(\eta)}(\Delta, \mathbf{k})(C_3^z)^{-1} = H^{(\eta)}(\Delta, C_3^z \mathbf{k})$. Here, $C_3^z \mathbf{k}$ is defined by the rotation matrix

$$C_3^z \begin{pmatrix} k_x \\ k_y \end{pmatrix} = \begin{pmatrix} \cos \vartheta & \sin \vartheta \\ -\sin \vartheta & \cos \vartheta \end{pmatrix} \begin{pmatrix} k_x \\ k_y \end{pmatrix}, \quad (\text{S26})$$

where $\vartheta = 2\pi/3$.

The C_3^z and \mathcal{M}_y symmetries imply that the system preserves reflection symmetry about other two axes with angle $\pm\pi/6$ with respect from the x -axis. Thus, for electric fields polarised parallel or normal to those two high-symmetry axes, the shift vector also acts as a pseudovector.

5. Stacking Dependence

Now we show that the shift vector switches sign when the stacking configuration is switched from AB to BA. AB/BA stacked BLG are related by flipping the sample about an axes along the armchair direction. For concreteness, we concentrate on the y -axis, so that this flip can be denoted $C_2^y : (x, y, z) \rightarrow (-x, y, -z)$ as the rotation about y -axis by π . We note that C_2^y not only flips the sample, but also interchanges the layer indices. As a result, the interlayer potential between the bottom and the top layer Δ switches sign. The real-space Hamiltonians of AB and BA stacked BLG satisfy $C_2^y \mathcal{H}^{(\text{AB})}(\Delta, \mathbf{r})(C_2^y)^{-1} = \mathcal{H}^{(\text{AB})}(\Delta, C_2^y \mathbf{r}) = \mathcal{H}^{(\text{BA})}(-\Delta, \mathbf{r})$. The Bloch Hamiltonians are thus related by $C_2^y H^{(\text{AB})}(\Delta, \mathbf{k})(C_2^y)^{-1} = H^{(\text{BA})}(-\Delta, C_2^y \mathbf{k})$. Here, we consider BLG as a 2D system with $\mathbf{k} = (k_x, k_y)$ and $C_2^y(k_x, k_y) = (-k_x, k_y) = \mathcal{M}_y(k_x, k_y)$. We note that the dispersion is independent of stacking configuration and interlayer potential direction $\epsilon_n^{(\text{AB})}(\Delta, \mathbf{k}) = \epsilon_n^{(\text{BA})}(-\Delta, \mathbf{k})$ and C_2^y satisfies $(C_2^y)^{-1} = C_2^y = (C_2^y)^\dagger$. It follows that the wavefunctions are related by

$$\epsilon_n^{(\text{AB})}(\Delta, \mathbf{k}) = \epsilon_n^{(\text{BA})}(-\Delta, C_2^y \mathbf{k}), \quad C_2^y |u_n^{(\text{AB})}(\Delta, \mathbf{k})\rangle = |u_n^{(\text{BA})}(-\Delta, C_2^y \mathbf{k})\rangle. \quad (\text{S27})$$

Thus we have

$$\langle u_m^{(\text{AB})}(\Delta, \mathbf{k}_1) | u_n^{(\text{AB})}(\Delta, \mathbf{k}_2) \rangle = \langle u_m^{(\text{AB})}(\Delta, \mathbf{k}_1) | (C_2^y)^{-1} C_2^y | u_n^{(\text{AB})}(\Delta, \mathbf{k}_2) \rangle = \langle u_m^{(\text{BA})}(-\Delta, C_2^y \mathbf{k}_1) | u_n^{(\text{BA})}(-\Delta, C_2^y \mathbf{k}_2) \rangle. \quad (\text{S28})$$

The velocity operators transform as $C_2^y \nu_x^{(AB)}(\Delta)(C_2^y)^{-1} = -\nu_x^{(BA)}(-\Delta)$ and $C_2^y \nu_y^{(AB)}(\Delta)(C_2^y)^{-1} = \nu_y^{(BA)}(-\Delta)$. Thus, for a linear polarisation angle θ , we have $C_2^y \nu_\theta^{(AB)}(\Delta)(C_2^y)^{-1} = \nu_{\pi-\theta}^{(BA)}(-\Delta)$. This gives

$$\begin{aligned} \langle u_m^{(AB)}(\Delta, \mathbf{k}_1) | \nu_\theta^{(AB)}(\Delta) | u_n^{(AB)}(\Delta, \mathbf{k}_2) \rangle &= \langle u_m^{(AB)}(\Delta, \mathbf{k}_1) | (C_2^y)^{-1} C_2^y \nu_\theta^{(AB)}(\Delta) (C_2^y)^{-1} | u_n^{(AB)}(\Delta, \mathbf{k}_2) \rangle \\ &= \langle u_m^{(BA)}(-\Delta, C_2^y \mathbf{k}_1) | \nu_{\pi-\theta}^{(BA)}(-\Delta) | u_n^{(BA)}(-\Delta, C_2^y \mathbf{k}_2) \rangle. \end{aligned} \quad (\text{S29})$$

We can perform the similar analysis on the Wilson line and the shift vector:

$$\mathcal{W}^{(AB)}(\Delta, \theta, \mathbf{k}, \mathbf{q}) = \mathcal{W}^{(BA)}(-\Delta, \pi - \theta, C_2^y \mathbf{k}, C_2^y \mathbf{q}), \quad \arg[\mathcal{W}^{(AB)}(\Delta, \theta, \mathbf{k}, \mathbf{q})] = \arg[\mathcal{W}^{(BA)}(-\Delta, \pi - \theta, C_2^y \mathbf{k}, C_2^y \mathbf{q})], \quad (\text{S30})$$

The shift vector can be calculated by taking the derivatives of $\arg[\mathcal{W}^{(\eta)}]$ in k -space. Noting the identity in Eq. (S21) that the shift vector is invariant for $\theta \rightarrow \theta + \pi$, we arrive at

$$r_x^{(AB)}(\Delta, \theta, \mathbf{k}) = -r_x^{(BA)}(-\Delta, -\theta, C_2^y \mathbf{k}), \quad r_y^{(AB)}(\Delta, \theta, \mathbf{k}) = r_y^{(BA)}(-\Delta, -\theta, C_2^y \mathbf{k}). \quad (\text{S31})$$

Noting that $\mathcal{M}_y C_2^y \mathbf{k} = \mathbf{k}$, and combining Eq. (S22) and (S31), we have

$$\mathbf{r}^{(AB)}(\Delta, \theta, \mathbf{k}) = \mathbf{r}^{(BA)}(-\Delta, \theta, \mathbf{k}). \quad (\text{S32})$$

Finally, recalling that the shift vector switches sign for $\Delta \rightarrow -\Delta$ [Eq. (S14)], thus we have

$$\mathbf{r}^{(AB)}(\Delta, \theta, \mathbf{k}) = -\mathbf{r}^{(BA)}(\Delta, \theta, \mathbf{k}). \quad (\text{S33})$$

Since the dispersion and $|\nu_\theta^{(\eta)}|^2$ are stacking independent, it follows that the shift currents flow in opposite directions in the two stacking configurations, as discussed in the main text.

B. Shift Vector Configuration Dependence for Staggered Sublattice Potential, e.g. G/hBN

We now examine the symmetry constraints of the shift vector in a gapped Dirac material with staggered sublattice potential difference described by the Bloch Hamiltonian $H(\delta, \mathbf{k})$, where δ is the sublattice potential difference and \mathbf{k} is the wavevector measured from the Γ point. In this section, we focus on the spinless fermions, which can be realised in a commensurate stacked graphene-hexagonal boron nitride (G/hBN) system, where the sign of δ depends on the alignment between the graphene and hBN layers. Such commensurate stacking have been achieved recently in G/hBN as evidenced by substantial gap opening at the charge neutrality point. For simplicity, we will consider the case whereby the carbon atoms in graphene are directly on top of the boron and nitrogen atoms in hBN (e.g., found within a single commensurate domain). In-plane rotation of the hBN layer by π (keeping the graphene layer fixed) leads to the interchange of the electric potential at the A and B site of graphene, thus reversing the sign of δ . In the following, we will show that the shift vector and SPC depend on the atomic alignment and light polarisation. For consistency of notation for the various vdW materials and systems considered here, we will fix the orientation so that one of the armchair directions is aligned along the y -direction (similar to that discussed for BLG above).

1. Time Reversal Symmetry

The system is invariant under time reversal operation: $\mathcal{T}H(\delta, \mathbf{k})\mathcal{T}^{-1} = H(\delta, -\mathbf{k})$. Thus the dispersion and the Bloch wavefunctions transform under \mathcal{T} as

$$\epsilon_n(\delta, \mathbf{k}) = \epsilon_n(\delta, -\mathbf{k}), \quad \mathcal{T}|u_n(\delta, \mathbf{k})\rangle = |u_n(\delta, -\mathbf{k})\rangle^*. \quad (\text{S34})$$

The above gives us

$$\langle u_m(\delta, \mathbf{k}_1) | u_n(\delta, \mathbf{k}_2) \rangle = \langle u_m(\delta, \mathbf{k}_1) | \mathcal{T}^{-1} \mathcal{T} | u_n(\delta, \mathbf{k}_2) \rangle = \langle u_m(\delta, -\mathbf{k}_1) | u_n(\delta, -\mathbf{k}_2) \rangle^*. \quad (\text{S35})$$

The velocity operator transforms as $\mathcal{T}\hat{v}(\delta)\mathcal{T}^{-1} = -\hat{v}(\delta)$. Thus, for a given polarisation angle θ , the velocity matrix element satisfies

$$\begin{aligned} \langle u_m(\delta, \mathbf{k}_1) | \nu_\theta(\delta) | u_n(\delta, \mathbf{k}_2) \rangle &= \langle u_m(\delta, \mathbf{k}_1) | \mathcal{T}^{-1} \mathcal{T} [\nu_x(\delta) \cos \theta + \nu_y(\delta) \sin \theta] \mathcal{T}^{-1} \mathcal{T} | u_n(\delta, \mathbf{k}_2) \rangle \\ &= -\langle u_m(\delta, -\mathbf{k}_1) | \nu_\theta(\delta) | u_n(\delta, -\mathbf{k}_2) \rangle^*. \end{aligned} \quad (\text{S36})$$

We obtain the symmetry constraint for the Wilson line:

$$\mathcal{W}(\delta, \theta, \mathbf{k}, \mathbf{q}) = -[\mathcal{W}(\delta, \theta, -\mathbf{k}, -\mathbf{q})]^*, \quad \arg[\mathcal{W}(\delta, \theta, \mathbf{k}, \mathbf{q})] = -\arg[\mathcal{W}(\delta, \theta, -\mathbf{k}, -\mathbf{q})] + \pi. \quad (\text{S37})$$

As a result, the shift vector in a time-reversal invariant system is even in k -space:

$$\mathbf{r}(\delta, \theta, \mathbf{k}) = \mathbf{r}(\delta, \theta, -\mathbf{k}). \quad (\text{S38})$$

2. Inversion

For $\delta \neq 0$, the system breaks inversion symmetry. Under inversion operation, the real space Hamiltonian satisfies $\mathcal{I}\mathcal{H}(\delta, \mathbf{r})\mathcal{I}^{-1} = \mathcal{H}(\delta, -\mathbf{r}) = \mathcal{H}(-\delta, \mathbf{r})$, i.e. inversion switches the staggered potential. As a result, the Bloch Hamiltonian transforms as $\mathcal{I}H(\delta, \mathbf{k})\mathcal{I}^{-1} = H(-\delta, -\mathbf{k})$, and the dispersion and Bloch wavefunction satisfy:

$$\epsilon_n(\delta, \mathbf{k}) = \epsilon_n(-\delta, -\mathbf{k}), \quad \mathcal{I}|u_n(\delta, \mathbf{k})\rangle = |u_n(-\delta, -\mathbf{k})\rangle. \quad (\text{S39})$$

Thus we have

$$\langle u_m(\delta, \mathbf{k}_1)|u_n(\delta, \mathbf{k}_2)\rangle = \langle u_m(\delta, \mathbf{k}_1)|\mathcal{I}^{-1}\mathcal{I}|u_n(\delta, \mathbf{k}_2)\rangle = \langle u_m(-\delta, -\mathbf{k}_1)|u_n(-\delta, -\mathbf{k}_2)\rangle. \quad (\text{S40})$$

On the other hand, the velocity operator transforms as $\mathcal{I}\hat{v}(\delta)\mathcal{I}^{-1} = -\hat{v}(-\delta)$. This yields

$$\begin{aligned} \langle u_m(\delta, \mathbf{k}_1)|\nu_\theta(\delta)|u_n(\delta, \mathbf{k}_2)\rangle &= \langle u_m(\delta, \mathbf{k}_1)|\mathcal{I}^{-1}\mathcal{I}\nu_\theta(\delta)\mathcal{I}^{-1}\mathcal{I}|u_n(\delta, \mathbf{k}_2)\rangle \\ &= -\langle u_m(-\delta, -\mathbf{k}_1)|\nu_\theta(-\delta)|u_n(-\delta, -\mathbf{k}_2)\rangle. \end{aligned} \quad (\text{S41})$$

We obtain the symmetry constraint for the Wilson line:

$$\mathcal{W}(\delta, \theta, \mathbf{k}, \mathbf{q}) = -\mathcal{W}(-\delta, \theta, -\mathbf{k}, -\mathbf{q}), \quad \arg[\mathcal{W}(\delta, \theta, \mathbf{k}, \mathbf{q})] = \arg[\mathcal{W}(-\delta, \theta, -\mathbf{k}, -\mathbf{q})] + \pi. \quad (\text{S42})$$

The shift vector obeys the following relation:

$$\mathbf{r}(\delta, \theta, \mathbf{k}) = -\mathbf{r}(-\delta, \theta, -\mathbf{k}). \quad (\text{S43})$$

Furthermore, we note that under time reversal symmetry, the shift vector is even in k -space. Eq. (S38) and (S43) demand that the shift vector switches sign when the sublattice potential difference is switched:

$$\mathbf{r}(\delta, \theta, \mathbf{k}) = -\mathbf{r}(-\delta, \theta, \mathbf{k}). \quad (\text{S44})$$

As a result, the direction of SPC is expected to be reversed when the sublattice potential difference is reversed. As we discussed, in G/hBN, this can be achieved by different alignment of hBN below the graphene layer, for example, by in-plane rotation of hBN by π . Thus SPC serves as a tool to determine the stacking alignment in G/hBN.

3. Mirror Symmetry

For consistency of notation for the various vdW materials and systems considered here, we will fix the orientation so that one of the armchair directions is aligned along the y -direction (similar to that discussed for BLG above). Mirror symmetry about the y -axis ensures: $\mathcal{M}_y\mathcal{H}(\delta, \mathbf{r})\mathcal{M}_y^{-1} = \mathcal{H}(\delta, \mathbf{r})$ and $\mathcal{M}_yH(\delta, \mathbf{k})\mathcal{M}_y^{-1} = H(\delta, \mathcal{M}_y\mathbf{k})$. Thus we have

$$\epsilon_n(\delta, \mathbf{k}) = \epsilon_n(\delta, \mathcal{M}_y\mathbf{k}), \quad \mathcal{M}_y|u_n(\delta, \mathbf{k})\rangle = |u_n(\delta, \mathcal{M}_y\mathbf{k})\rangle, \quad (\text{S45})$$

and

$$\langle u_m(\delta, \mathbf{k}_1)|u_n(\delta, \mathbf{k}_2)\rangle = \langle u_m(\delta, \mathbf{k}_1)|\mathcal{M}_y^{-1}\mathcal{M}_y|u_n(\delta, \mathbf{k}_2)\rangle = \langle u_m(\delta, \mathcal{M}_y\mathbf{k}_1)|u_n(\delta, \mathcal{M}_y\mathbf{k}_2)\rangle. \quad (\text{S46})$$

The velocity operators transform as $\mathcal{M}_y\nu_x(\delta)\mathcal{M}_y^{-1} = -\nu_x(\delta)$ and $\mathcal{M}_y\nu_y(\delta)\mathcal{M}_y^{-1} = \nu_y(\delta)$, thus we have $\mathcal{M}_y\nu_\theta^{(n)}\mathcal{M}_y^{-1} = \nu_{\pi-\theta}(\delta)$. This gives

$$\begin{aligned} \langle u_m(\delta, \mathbf{k}_1)|\nu_\theta(\delta)|u_n(\delta, \mathbf{k}_2)\rangle &= \langle u_m(\delta, \mathbf{k}_1)|\mathcal{M}_y^{-1}\mathcal{M}_y\nu_\theta(\delta)\mathcal{M}_y^{-1}\mathcal{M}_y|u_n(\delta, \mathbf{k}_2)\rangle \\ &= \langle u_m(\delta, \mathcal{M}_y\mathbf{k}_1)|\nu_{\pi-\theta}(\delta)|u_n(\delta, \mathcal{M}_y\mathbf{k}_2)\rangle. \end{aligned} \quad (\text{S47})$$

The Wilson line satisfies

$$\mathcal{W}(\delta, \theta, \mathbf{k}, \mathbf{q}) = \mathcal{W}(\delta, \pi - \theta, \mathcal{M}_y \mathbf{k}, \mathcal{M}_y \mathbf{q}), \quad \arg[\mathcal{W}(\delta, \theta, \mathbf{k}, \mathbf{q})] = \arg[\mathcal{W}(\delta, \pi - \theta, \mathcal{M}_y \mathbf{k}, \mathcal{M}_y \mathbf{q})], \quad (\text{S48})$$

and shift vector thus satisfies

$$r_x(\delta, \theta, \mathbf{k}) = -r_x(\delta, \pi - \theta, \mathcal{M}_y \mathbf{k}), \quad r_y(\delta, \theta, \mathbf{k}) = r_y(\delta, \pi - \theta, \mathcal{M}_y \mathbf{k}). \quad (\text{S49})$$

We note that the electric field polarisation along $\hat{\mathbf{e}}_\theta$ is equivalent to the polarisation along $-\hat{\mathbf{e}}_\theta = \hat{\mathbf{e}}_{\pi+\theta}$. Thus Eq. (S49) can be rewritten as

$$r_x(\delta, \theta, \mathbf{k}) = -r_x(\delta, -\theta, \mathcal{M}_y \mathbf{k}), \quad r_y(\delta, \theta, \mathbf{k}) = r_y(\delta, -\theta, \mathcal{M}_y \mathbf{k}). \quad (\text{S50})$$

Additionally, following the similar analysis in Eq. (S23), we combine the constraints of time reversal symmetry [Eq. (S38)] and mirror symmetry [Eq. (S50)] to obtain

$$r_x(\delta, \theta, \mathbf{k}) = -r_x(\delta, -\theta, k_x, -k_y), \quad r_y(\delta, \theta, \mathbf{k}) = r_y(\delta, -\theta, k_x, -k_y). \quad (\text{S51})$$

Similar with the scenario of Bernal stacked BLG, the shift vector in Eq. (S51) also exhibits pseudovector property when the electric field polarisation is either perpendicular to ($\theta = 0, \pi$) or parallel with ($\theta = \pm\pi/2$) with mirror plane (y -axis). At these polarisations, $r_x(\delta, \theta, \mathbf{k})$ flips sign for $k_y \rightarrow -k_y$ while $r_y(\delta, \theta, \mathbf{k})$ remains invariant. Thus, integration over the k -space in Eq. (2) in the main text leads to transverse (longitudinal) SPC for linear polarisations perpendicular to (parallel with) the mirror reflection axis.

Furthermore, the material under consideration is also invariant under three-fold in-plane rotational symmetry C_3^z like BLG. Thus the system possesses three mirror reflection axes with angle $\pi/2, \pm\pi/6$. Similar argument can be applied to the shift vector and shift current after rotating the system by $2\pi/3$ about the z axis, and we expect transverse (longitudinal) SPC for polarisations perpendicular to (parallel with) any of the mirror reflection axes.

C. Shift Vector Configuration Dependence for Monolayer TMDs

Now we consider the configuration dependence of shift vector in monolayer TMDs, which possess hexagonal lattice structure with A and B lattice site hosting different atoms. Thus they have sublattice potential difference δ . Further, large Ising spin-orbit coupling yields spin-valley locked states. In the following, we show that the spin SPC in these materials depends on the δ and the incident light polarisation.

1. Time Reversal Symmetry

Monolayer TMDs are invariant under time reversal symmetry $\mathcal{T}H(\delta, \mathbf{k})\mathcal{T}^{-1} = H(\delta, -\mathbf{k})$ and the Bloch wavefunction projected to each spin state transforms as

$$\epsilon_n^s(\delta, \mathbf{k}) = \epsilon_n^{-s}(\delta, -\mathbf{k}), \quad \mathcal{T}|u_n^s(\delta, \mathbf{k})\rangle = |u_n^{-s}(\delta, -\mathbf{k})\rangle^*, \quad (\text{S52})$$

where $s = \uparrow, \downarrow$ denotes the z component of the electron spin (arising from the large Ising spin-orbit coupling in the valleys of TMDs). The above wavefunction transformation yields

$$\langle u_m^{s_1}(\delta, \mathbf{k}_1) | u_n^{s_2}(\delta, \mathbf{k}_2) \rangle = \langle u_m^{s_1}(\delta, \mathbf{k}_1) | \mathcal{T}^{-1} \mathcal{T} | u_n^{s_2}(\delta, \mathbf{k}_2) \rangle = \langle u_m^{-s_1}(\delta, -\mathbf{k}_1) | u_n^{-s_2}(\delta, -\mathbf{k}_2) \rangle^*. \quad (\text{S53})$$

The velocity operator transforms as $\mathcal{T}\hat{v}(\delta)\mathcal{T}^{-1} = -\hat{v}(\delta)$. Thus, for a given polarisation angle θ , the velocity matrix element satisfies

$$\begin{aligned} \langle u_m^{s_1}(\delta, \mathbf{k}_1) | \nu_\theta(\delta) | u_n^{s_2}(\delta, \mathbf{k}_2) \rangle &= \langle u_m^{s_1}(\delta, \mathbf{k}_1) | \mathcal{T}^{-1} \mathcal{T} \nu_\theta(\delta) \mathcal{T}^{-1} \mathcal{T} | u_n^{s_2}(\delta, \mathbf{k}_2) \rangle \\ &= -\langle u_m^{-s_1}(\delta, -\mathbf{k}_1) | \nu_\theta(\delta) | u_n^{-s_2}(\delta, -\mathbf{k}_2) \rangle^*. \end{aligned} \quad (\text{S54})$$

We obtain the symmetry constraint for the Wilson line:

$$\mathcal{W}^s(\delta, \theta, \mathbf{k}, \mathbf{q}) = -[\mathcal{W}^{-s}(\delta, \theta, -\mathbf{k}, -\mathbf{q})]^*, \quad \arg[\mathcal{W}^s(\delta, \theta, \mathbf{k}, \mathbf{q})] = -\arg[\mathcal{W}^{-s}(\delta, \theta, -\mathbf{k}, -\mathbf{q})] + \pi. \quad (\text{S55})$$

As a result, the spin-dependent shift vector in a time-reversal invariant system satisfies

$$\mathbf{r}^s(\delta, \theta, \mathbf{k}) = \mathbf{r}^{-s}(\delta, \theta, -\mathbf{k}). \quad (\text{S56})$$

Due to the large (Ising) spin-valley locking in TMDs for photon energies close to the bandgap, we anticipate that this spin SPC is locked to each of the valleys. However, the spin-resolved shift vectors have the same sign [see Eq. (S56), albeit at opposite \mathbf{k}]. Since the square of the velocity matrix element is even under $\mathbf{k} \rightarrow -\mathbf{k}$ and $s \rightarrow -s$ [Eq. (S54)], the weighted shift vector satisfies $\mathbf{R}^s(\delta, \theta, \mathbf{k}) = \mathbf{R}^{-s}(\delta, \theta, -\mathbf{k})$. Thus, upon integration over the k -space, both \uparrow, \downarrow spin SPC move in the same direction yielding a charge current.

2. Inversion

Due to the sublattice potential difference δ , monolayer TMDs also break inversion symmetry. Under spatial inversion operation, we have $\mathcal{I}\mathcal{H}(\delta, \mathbf{r})\mathcal{I}^{-1} = \mathcal{H}(-\delta, \mathbf{r})$ and $\mathcal{I}H(\delta, \mathbf{k})\mathcal{I}^{-1} = H(-\delta, -\mathbf{k})$. On the other hand, spin is invariant under inversion. Thus the spin resolved Bloch wavefunction satisfies

$$\epsilon_n^s(\delta, \mathbf{k}) = \epsilon_n^s(-\delta, -\mathbf{k}), \quad \mathcal{I}|u_n^s(\delta, \mathbf{k})\rangle = |u_n^s(-\delta, -\mathbf{k})\rangle. \quad (\text{S57})$$

Thus we have

$$\langle u_m^{s_1}(\delta, \mathbf{k}_1) | u_n^{s_2}(\delta, \mathbf{k}_2) \rangle = \langle u_m^{s_1}(\delta, \mathbf{k}_1) | \mathcal{I}^{-1} \mathcal{I} | u_n^{s_2}(\delta, \mathbf{k}_2) \rangle = \langle u_m^{s_1}(-\delta, -\mathbf{k}_1) | u_n^{s_2}(-\delta, -\mathbf{k}_2) \rangle. \quad (\text{S58})$$

The velocity operator transforms as $\mathcal{I}\hat{v}(\delta)\mathcal{I}^{-1} = -\hat{v}(-\delta)$. This yields

$$\begin{aligned} \langle u_m^{s_1}(\delta, \mathbf{k}_1) | \nu_\theta(\delta) | u_n^{s_2}(\delta, \mathbf{k}_2) \rangle &= \langle u_m^{s_1}(\delta, \mathbf{k}_1) | \mathcal{I}^{-1} \mathcal{I} \nu_\theta(\delta) \mathcal{I}^{-1} \mathcal{I} | u_n^{s_2}(\delta, \mathbf{k}_2) \rangle \\ &= -\langle u_m^{s_1}(-\delta, -\mathbf{k}_1) | \nu_\theta(-\delta) | u_n^{s_2}(-\delta, -\mathbf{k}_2) \rangle. \end{aligned} \quad (\text{S59})$$

We obtain the symmetry constraint for the Wilson line:

$$\mathcal{W}^s(\delta, \theta, \mathbf{k}, \mathbf{q}) = -\mathcal{W}^s(-\delta, \theta, -\mathbf{k}, -\mathbf{q}), \quad \arg[\mathcal{W}^s(\delta, \theta, \mathbf{k}, \mathbf{q})] = \arg[\mathcal{W}^s(-\delta, \theta, -\mathbf{k}, -\mathbf{q})] + \pi. \quad (\text{S60})$$

As a result, the shift vector obeys the following relation:

$$\mathbf{r}^s(\delta, \theta, \mathbf{k}) = -\mathbf{r}^s(-\delta, \theta, -\mathbf{k}). \quad (\text{S61})$$

The spin SPC can be obtained by integrating the weighted shift vector over the entire k -space [Eq. (2) in the main text], thus Eq. (S61) requires that the spin resolved SPC reverses sign for $\delta \rightarrow -\delta$. Furthermore, the charge current can be calculated by summing over the spin SPC and also flips sign for $\delta \rightarrow -\delta$.

3. Mirror Symmetry

Monolayer TMD also exhibits mirror symmetry about the y -axis: $\mathcal{M}_y\mathcal{H}(\delta, \mathbf{r})\mathcal{M}_y^{-1} = \mathcal{H}(\delta, \mathbf{r})$ and $\mathcal{M}_yH(\delta, \mathbf{k})\mathcal{M}_y^{-1} = H(\delta, \mathcal{M}_y\mathbf{k})$. On the other hand, spin transforms in the same way as angular momentum upon reflection. In 3D, for a yz mirror plane, the z component of the spin flips sign under $\mathcal{M}_y : (x, y, z) \rightarrow (-x, y, -z)$. Thus the wavefunction projected to each spin satisfies

$$\epsilon_n^s(\delta, \mathbf{k}) = \epsilon_n^{-s}(\delta, \mathcal{M}_y\mathbf{k}), \quad \mathcal{M}_y|u_n^s(\delta, \mathbf{k})\rangle = |u_n^{-s}(\delta, \mathcal{M}_y\mathbf{k})\rangle, \quad (\text{S62})$$

and

$$\langle u_m^{s_1}(\delta, \mathbf{k}_1) | u_n^{s_2}(\delta, \mathbf{k}_2) \rangle = \langle u_m^{s_1}(\delta, \mathbf{k}_1) | \mathcal{M}_y^{-1} \mathcal{M}_y | u_n^{s_2}(\delta, \mathbf{k}_2) \rangle = \langle u_m^{-s_1}(\delta, \mathcal{M}_y\mathbf{k}_1) | u_n^{-s_2}(\delta, \mathcal{M}_y\mathbf{k}_2) \rangle. \quad (\text{S63})$$

The velocity operators transform as $\mathcal{M}_y\nu_x(\delta)\mathcal{M}_y^{-1} = -\nu_x(\delta)$ and $\mathcal{M}_y\nu_y(\delta)\mathcal{M}_y^{-1} = \nu_y(\delta)$, thus we have $\mathcal{M}_y\nu_\theta(\delta)\mathcal{M}_y^{-1} = \nu_{\pi-\theta}(\delta)$. This gives

$$\begin{aligned} \langle u_m^{s_1}(\delta, \mathbf{k}_1) | \nu_\theta(\delta) | u_n^{s_2}(\delta, \mathbf{k}_2) \rangle &= \langle u_m^{s_1}(\delta, \mathbf{k}_1) | \mathcal{M}_y^{-1} \mathcal{M}_y \nu_\theta(\delta) \mathcal{M}_y^{-1} \mathcal{M}_y | u_n^{s_2}(\delta, \mathbf{k}_2) \rangle \\ &= \langle u_m^{-s_1}(\delta, \mathcal{M}_y\mathbf{k}_1) | \nu_{\pi-\theta}(\delta) | u_n^{-s_2}(\delta, \mathcal{M}_y\mathbf{k}_2) \rangle. \end{aligned} \quad (\text{S64})$$

The spin-dependent Wilson line satisfies

$$\mathcal{W}^s(\delta, \theta, \mathbf{k}, \mathbf{q}) = \mathcal{W}^{-s}(\delta, \pi - \theta, \mathcal{M}_y \mathbf{k}, \mathcal{M}_y \mathbf{q}), \quad \arg[\mathcal{W}^s(\delta, \theta, \mathbf{k}, \mathbf{q})] = \arg[\mathcal{W}^{-s}(\delta, \pi - \theta, \mathcal{M}_y \mathbf{k}, \mathcal{M}_y \mathbf{q})], \quad (\text{S65})$$

and shift vector obeys

$$r_x^s(\delta, \theta, \mathbf{k}) = -r_x^{-s}(\delta, \pi - \theta, \mathcal{M}_y \mathbf{k}), \quad r_y^s(\delta, \theta, \mathbf{k}) = r_y^{-s}(\delta, \pi - \theta, \mathcal{M}_y \mathbf{k}). \quad (\text{S66})$$

Since the polarisation directions θ and $\theta + \pi$ are equivalent, Eq. (S66) as

$$r_x^s(\delta, \theta, \mathbf{k}) = -r_x^{-s}(\delta, -\theta, \mathcal{M}_y \mathbf{k}), \quad r_y^s(\delta, \theta, \mathbf{k}) = r_y^{-s}(\delta, -\theta, \mathcal{M}_y \mathbf{k}). \quad (\text{S67})$$

Combining with Eq. (S56), we obtain the shift vector symmetry constraint for each spin:

$$r_x^s(\delta, \theta, \mathbf{k}) = -r_x^s(\delta, -\theta, k_x, -k_y), \quad r_y^s(\delta, \theta, \mathbf{k}) = r_y^s(\delta, -\theta, k_x, -k_y). \quad (\text{S68})$$

Similar to the charge current in BLG and G/hBN, the spin SPC is sensitive to the linear polarisation of light. For electric field polarised perpendicular to ($\theta = 0, \pi$) or parallel with ($\theta = \pm\pi/2$) the mirror axis, $r_x^s(\delta, \theta, \mathbf{k})$ flips sign for $k_y \rightarrow -k_y$ while $r_y^s(\delta, \theta, \mathbf{k})$ is invariant. This leads to transverse (longitudinal) spin SPC for polarisation perpendicular to (parallel with) the mirror axis. Since Eq. (S68) is valid for both spins, we anticipate that the charge SPC also exhibits the same polarisation dependence, i.e. the charge SPC is transverse (longitudinal) for electric field polarisation normal to (parallel with) the mirror plane.

Furthermore, monolayer TMDs are also invariant under C_3^z and possesses three mirror reflection axes that are separated by $\pm 2\pi/3$ apart from each other. Thus a similar argument on the polarisation dependent spin and charge SPC can be extended to other mirror reflection axes after rotating by $\pm 2\pi/3$ about the z -axis.

D. Shift Vector Configuration Dependence for 2H Stacked Bilayer TMDs

SPC in bilayer TMDs exhibits stacking and polarisation dependence as well. Here we focus on the most common 2H stacking configuration for bilayer TMDs, whereby one of the layers is rotated by π about the z -axis and then directly stacked on top of the other. In this stacking configuration, the A (B) site of the top layer is directly on top of the B (A) site of the bottom layer. We describe the system with a real space Hamiltonian $\mathcal{H}(\Delta, \delta, \mathbf{r})$, where Δ is the interlayer potential difference provided by an external out-of-plane electric field, and δ is the sublattice potential difference between A and B sites. In the absence of interlayer potential difference, the material is centrosymmetric and the SPC vanishes. Here we consider the symmetry constraints of the spin dependent shift vector and SPC when $\Delta \neq 0$.

1. Time Reversal Symmetry

Time reversal symmetry demands $\mathcal{T}H(\Delta, \delta, \mathbf{k})\mathcal{T}^{-1} = H(\Delta, \delta, -\mathbf{k})$. Thus the wavefunction projected to each spin satisfies

$$\epsilon_n^s(\Delta, \delta, \mathbf{k}) = \epsilon_n^{-s}(\Delta, \delta, -\mathbf{k}), \quad \mathcal{T}|u_n^s(\Delta, \delta, \mathbf{k})\rangle = |u_n^{-s}(\Delta, \delta, -\mathbf{k})\rangle^*, \quad (\text{S69})$$

and

$$\langle u_m^{s_1}(\Delta, \delta, \mathbf{k}_1) | u_n^{s_2}(\Delta, \delta, \mathbf{k}_2) \rangle = \langle u_m^{s_1}(\Delta, \delta, \mathbf{k}_1) | \mathcal{T}^{-1} \mathcal{T} | u_n^{s_2}(\Delta, \delta, \mathbf{k}_2) \rangle = \langle u_m^{-s_1}(\Delta, \delta, -\mathbf{k}_1) | u_n^{-s_2}(\Delta, \delta, -\mathbf{k}_2) \rangle^*. \quad (\text{S70})$$

Here, $s = \uparrow, \downarrow$ denotes the the electron spin along the z -axis.

The velocity operator transforms as $\mathcal{T}\hat{v}(\Delta, \delta)\mathcal{T}^{-1} = -\hat{v}(\Delta, \delta)$. Thus, for a given polarisation angle θ , the velocity matrix element satisfies

$$\begin{aligned} \langle u_m^{s_1}(\Delta, \delta, \mathbf{k}_1) | \nu_\theta(\Delta, \delta) | u_n^{s_2}(\Delta, \delta, \mathbf{k}_2) \rangle &= \langle u_m^{s_1}(\Delta, \delta, \mathbf{k}_1) | \mathcal{T}^{-1} \mathcal{T} \nu_\theta(\Delta, \delta) \mathcal{T}^{-1} \mathcal{T} | u_n^{s_2}(\Delta, \delta, \mathbf{k}_2) \rangle \\ &= -\langle u_m^{-s_1}(\Delta, \delta, -\mathbf{k}_1) | \nu_\theta(\Delta, \delta) | u_n^{-s_2}(\Delta, \delta, -\mathbf{k}_2) \rangle^*. \end{aligned} \quad (\text{S71})$$

We obtain the symmetry constraint for the Wilson line:

$$\mathcal{W}^s(\Delta, \delta, \theta, \mathbf{k}, \mathbf{q}) = -[\mathcal{W}^{-s}(\Delta, \delta, \theta, -\mathbf{k}, -\mathbf{q})]^*, \quad \arg[\mathcal{W}^s(\Delta, \delta, \theta, \mathbf{k}, \mathbf{q})] = -\arg[\mathcal{W}^{-s}(\Delta, \delta, \theta, -\mathbf{k}, -\mathbf{q})] + \pi. \quad (\text{S72})$$

As a result, the spin-dependent shift vector satisfies

$$\mathbf{r}^s(\Delta, \delta, \theta, \mathbf{k}) = \mathbf{r}^{-s}(\Delta, \delta, \theta, -\mathbf{k}). \quad (\text{S73})$$

Similar with the scenario in a monolayer TMD as discussed in the previous subsection, Eq. (S73) leads to spin SPC that is locked to each valley. We also note that the (weighted) shift vectors for opposite spins have the same sign at opposite \mathbf{k} . Thus the spin currents for $s = \uparrow, \downarrow$ flow in the same direction, leading to a net charge SPC.

2. Inversion

Under spatial inversion, the atomic configuration of the 2H stacked bilayer TMD remains invariant, while the interlayer potential flips sign: $\mathcal{I}\mathcal{H}(\Delta, \delta, \mathbf{r})\mathcal{I}^{-1} = \mathcal{H}(-\Delta, \delta, \mathbf{r})$. The Bloch Hamiltonian thus satisfies $\mathcal{I}H(\Delta, \delta, \mathbf{k})\mathcal{I}^{-1} = H(-\Delta, \delta, -\mathbf{k})$. This gives

$$\epsilon_n^s(\Delta, \delta, \mathbf{k}) = \epsilon_n^s(-\Delta, \delta, -\mathbf{k}), \quad \mathcal{I}|u_n^s(\Delta, \delta, \mathbf{k})\rangle = |u_n^s(-\Delta, \delta, -\mathbf{k})\rangle, \quad (\text{S74})$$

and

$$\langle u_m^{s_1}(\Delta, \delta, \mathbf{k}_1) | u_n^{s_2}(\Delta, \delta, \mathbf{k}_2) \rangle = \langle u_m^{s_1}(\Delta, \delta, \mathbf{k}_1) | \mathcal{I}^{-1} \mathcal{I} | u_n^{s_2}(\Delta, \delta, \mathbf{k}_2) \rangle = \langle u_m^{s_1}(-\Delta, \delta, -\mathbf{k}_1) | u_n^{s_2}(-\Delta, \delta, -\mathbf{k}_2) \rangle. \quad (\text{S75})$$

Upon spatial inversion, the velocity operator transforms as $\mathcal{I}\hat{v}(\Delta, \delta)\mathcal{I}^{-1} = -\hat{v}(-\Delta, \delta)$. This gives

$$\begin{aligned} \langle u_m^{s_1}(\Delta, \delta, \mathbf{k}_1) | \nu_\theta(\Delta, \delta) | u_n^{s_2}(\Delta, \delta, \mathbf{k}_2) \rangle &= \langle u_m^{s_1}(\Delta, \delta, \mathbf{k}_1) | \mathcal{I}^{-1} \mathcal{I} \nu_\theta(\Delta, \delta) \mathcal{I}^{-1} | u_n^{s_2}(\Delta, \delta, \mathbf{k}_2) \rangle \\ &= -\langle u_m^{s_1}(-\Delta, \delta, -\mathbf{k}_1) | \nu_\theta(-\Delta, \delta) | u_n^{s_2}(-\Delta, \delta, -\mathbf{k}_2) \rangle. \end{aligned} \quad (\text{S76})$$

It follows that the Wilson line satisfies

$$\mathcal{W}^s(\Delta, \delta, \theta, \mathbf{k}, \mathbf{q}) = -\mathcal{W}^s(-\Delta, \delta, \theta, -\mathbf{k}, -\mathbf{q}), \quad \arg[\mathcal{W}^s(\Delta, \delta, \theta, \mathbf{k}, \mathbf{q})] = \arg[\mathcal{W}^s(-\Delta, \delta, \theta, -\mathbf{k}, -\mathbf{q})] + \pi. \quad (\text{S77})$$

As a result, the spin-dependent shift vector satisfies

$$\mathbf{r}^s(\Delta, \delta, \theta, \mathbf{k}) = -\mathbf{r}^s(-\Delta, \delta, \theta, -\mathbf{k}). \quad (\text{S78})$$

Since the SPC is obtained by integrating the weighted shift vector and both $\rho(\Delta, \delta, \mathbf{k})$ and $|\nu_\theta(\Delta, \delta, \mathbf{k})|^2$ are even in Δ and \mathbf{k} , Eq. (S78) implies that the spin SPC flips direction for $\Delta \rightarrow -\Delta$. The charge SPC can be obtained by summing over $s = \uparrow, \downarrow$ and thus also reverses its direction upon reversing interlayer potential difference.

3. Mirror Symmetry

2H bilayer TMD is invariant under mirror reflection about the y axis: $\mathcal{M}_y H(\Delta, \delta, \mathbf{k}) \mathcal{M}_y^{-1} = H(\Delta, \delta, \mathcal{M}_y \mathbf{k})$. The spin acts as a pseudovector upon reflection, and thus s flips sign under \mathcal{M}_y . This leads to

$$\epsilon_n^s(\Delta, \delta, \mathbf{k}) = \epsilon_n^{-s}(\Delta, \delta, \mathcal{M}_y \mathbf{k}), \quad \mathcal{M}_y |u_n^s(\Delta, \delta, \mathbf{k})\rangle = |u_n^{-s}(\Delta, \delta, \mathcal{M}_y \mathbf{k})\rangle, \quad (\text{S79})$$

and

$$\langle u_m^{s_1}(\Delta, \delta, \mathbf{k}_1) | u_n^{s_2}(\Delta, \delta, \mathbf{k}_2) \rangle = \langle u_m^{s_1}(\Delta, \delta, \mathbf{k}_1) | \mathcal{M}_y^{-1} \mathcal{M}_y | u_n^{s_2}(\Delta, \delta, \mathbf{k}_2) \rangle = \langle u_m^{-s_1}(\Delta, \delta, \mathcal{M}_y \mathbf{k}_1) | u_n^{-s_2}(\Delta, \delta, \mathcal{M}_y \mathbf{k}_2) \rangle. \quad (\text{S80})$$

The velocity operators transform as $\mathcal{M}_y \nu_x(\Delta, \delta) \mathcal{M}_y^{-1} = -\nu_x(\Delta, \delta)$ and $\mathcal{M}_y \nu_y(\Delta, \delta) \mathcal{M}_y^{-1} = \nu_y(\Delta, \delta)$, thus we have $\mathcal{M}_y \nu_\theta(\Delta, \delta) \mathcal{M}_y^{-1} = \nu_{\pi-\theta}(\Delta, \delta)$. This gives

$$\begin{aligned} \langle u_m^{s_1}(\Delta, \delta, \mathbf{k}_1) | \nu_\theta(\Delta, \delta) | u_n^{s_2}(\Delta, \delta, \mathbf{k}_2) \rangle &= \langle u_m^{s_1}(\Delta, \delta, \mathbf{k}_1) | \mathcal{M}_y^{-1} \mathcal{M}_y \nu_\theta(\Delta, \delta) \mathcal{M}_y^{-1} \mathcal{M}_y | u_n^{s_2}(\Delta, \delta, \mathbf{k}_2) \rangle \\ &= \langle u_m^{-s_1}(\Delta, \delta, \mathcal{M}_y \mathbf{k}_1) | \nu_{\pi-\theta}(\Delta, \delta) | u_n^{-s_2}(\Delta, \delta, \mathcal{M}_y \mathbf{k}_2) \rangle. \end{aligned} \quad (\text{S81})$$

The spin-dependent Wilson line satisfies

$$\mathcal{W}^s(\Delta, \delta, \theta, \mathbf{k}, \mathbf{q}) = \mathcal{W}^{-s}(\Delta, \delta, \pi - \theta, \mathcal{M}_y \mathbf{k}, \mathcal{M}_y \mathbf{q}), \quad \arg[\mathcal{W}^s(\Delta, \delta, \theta, \mathbf{k}, \mathbf{q})] = \arg[\mathcal{W}^{-s}(\Delta, \delta, \pi - \theta, \mathcal{M}_y \mathbf{k}, \mathcal{M}_y \mathbf{q})], \quad (\text{S82})$$

and shift vector obeys

$$r_x^s(\Delta, \delta, \theta, \mathbf{k}) = -r_x^{-s}(\Delta, \delta, \pi - \theta, \mathcal{M}_y \mathbf{k}), \quad r_y^s(\Delta, \delta, \theta, \mathbf{k}) = r_y^{-s}(\Delta, \delta, \pi - \theta, \mathcal{M}_y \mathbf{k}). \quad (\text{S83})$$

Again, we use the identity that the polarisation directions θ and $\theta + \pi$ are equivalent to obtain

$$r_x^s(\Delta, \delta, \theta, \mathbf{k}) = -r_x^{-s}(\Delta, \delta, -\theta, \mathcal{M}_y \mathbf{k}), \quad r_y^s(\Delta, \delta, \theta, \mathbf{k}) = r_y^{-s}(\Delta, \delta, -\theta, \mathcal{M}_y \mathbf{k}). \quad (\text{S84})$$

Combining with Eq. (S73), we obtain the shift vector symmetry constraint for each spin:

$$r_x^s(\Delta, \delta, \theta, \mathbf{k}) = -r_x^{-s}(\Delta, \delta, -\theta, k_x, -k_y), \quad r_y^s(\Delta, \delta, \theta, \mathbf{k}) = r_y^{-s}(\Delta, \delta, -\theta, k_x, -k_y). \quad (\text{S85})$$

Eq. (S85) ensures that for polarisation angles $\theta = 0, \pi$ and $\theta = \pm\pi/2$, $r_x^s(\Delta, \delta, \theta, \mathbf{k})$ is odd under $k_y \rightarrow -k_y$ while $r_y^s(\Delta, \delta, \theta, \mathbf{k})$ is even. Thus, for electric field polarised perpendicular to (parallel with) with mirror reflection axis, the spin SPC is transverse (longitudinal). Again, similar with the scenario in a monolayer TMD, since the symmetry constraint in Eq. (S85) is valid for both spins, the charge SPC exhibits the same polarisation dependence as the spin SPC.

We remark that 2H stacked bilayer TMD also possesses three-fold in-plane rotational symmetry C_3^z and thus has two more mirror axes that are separated $\pm 2\pi/3$ from the y -axis. The argument above on polarisation dependent spin and charge SPC can also be applied to the other two mirror axes after rotating the coordinate system by $\pm 2\pi/3$.

Now we move on to \mathcal{M}_x . 2H stacked bilayer TMD breaks mirror symmetry with respect to the x -axis. \mathcal{M}_x interchanges the A, B sublattice sites, thus reversing δ : $\mathcal{M}_x \mathcal{H}(\Delta, \delta, \mathbf{r}) \mathcal{M}_x = \mathcal{H}(\Delta, -\delta, \mathbf{r})$. The Bloch Hamiltonian satisfies $\mathcal{M}_x H(\Delta, \delta, \mathbf{k}) \mathcal{M}_x = H(\Delta, -\delta, \mathcal{M}_x \mathbf{k})$. For wavefunctions projected to each spin state, under mirror reflection, the spin transforms as a pseudovector and the z component s flips sign. Thus we have

$$\epsilon_n^s(\Delta, \delta, \mathbf{k}) = \epsilon_n^{-s}(\Delta, -\delta, \mathcal{M}_x \mathbf{k}), \quad \mathcal{M}_x |u_n^s(\Delta, \delta, \mathbf{k})\rangle = |u_n^{-s}(\Delta, -\delta, \mathcal{M}_x \mathbf{k})\rangle, \quad (\text{S86})$$

and

$$\langle u_m^{s_1}(\Delta, \delta, \mathbf{k}_1) | u_n^{s_2}(\Delta, \delta, \mathbf{k}_2) \rangle = \langle u_m^{s_1}(\Delta, \delta, \mathbf{k}_1) | \mathcal{M}_x^{-1} \mathcal{M}_x | u_n^{s_2}(\Delta, \delta, \mathbf{k}_2) \rangle = \langle u_m^{-s_1}(\Delta, -\delta, \mathcal{M}_x \mathbf{k}_1) | u_n^{-s_2}(\Delta, -\delta, \mathcal{M}_x \mathbf{k}_2) \rangle. \quad (\text{S87})$$

Under \mathcal{M}_x , the y component of the velocity operator switches sign $\mathcal{M}_x \nu_y(\Delta, \delta) \mathcal{M}_x^{-1} = -\nu_y(\Delta, -\delta)$ while the x component is invariant $\mathcal{M}_x \nu_x(\Delta, \delta) \mathcal{M}_x^{-1} = \nu_x(\Delta, -\delta)$. Thus for a given polarisation θ , we have $\mathcal{M}_x \nu_\theta(\Delta, \delta) \mathcal{M}_x^{-1} = \nu_{-\theta}(\Delta, -\delta)$ and

$$\begin{aligned} \langle u_m^{s_1}(\Delta, \delta, \mathbf{k}_1) | \nu_\theta(\Delta, \delta) | u_n^{s_2}(\Delta, \delta, \mathbf{k}_2) \rangle &= \langle u_m^{s_1}(\Delta, \delta, \mathbf{k}_1) | \mathcal{M}_x^{-1} \mathcal{M}_x \nu_\theta(\Delta, \delta) \mathcal{M}_x^{-1} \mathcal{M}_x | u_n^{s_2}(\Delta, \delta, \mathbf{k}_2) \rangle \\ &= \langle u_m^{-s_1}(\Delta, -\delta, \mathcal{M}_x \mathbf{k}_1) | \nu_{-\theta}(\Delta, -\delta) | u_n^{-s_2}(\Delta, -\delta, \mathcal{M}_x \mathbf{k}_2) \rangle. \end{aligned} \quad (\text{S88})$$

Thus the Wilson line satisfies

$$\mathcal{W}^s(\Delta, \delta, \theta, \mathbf{k}, \mathbf{q}) = \mathcal{W}^{-s}(\Delta, -\delta, -\theta, \mathcal{M}_x \mathbf{k}, \mathcal{M}_x \mathbf{q}), \quad \arg[\mathcal{W}^s(\Delta, \delta, \theta, \mathbf{k}, \mathbf{q})] = \arg[\mathcal{W}^{-s}(\Delta, -\delta, -\theta, \mathcal{M}_x \mathbf{k}, \mathcal{M}_x \mathbf{q})], \quad (\text{S89})$$

The spin dependent shift vector satisfies

$$r_x^s(\Delta, \delta, \theta, \mathbf{k}) = r_x^{-s}(\Delta, -\delta, -\theta, \mathcal{M}_x \mathbf{k}), \quad r_y^s(\Delta, \delta, \theta, \mathbf{k}) = -r_y^{-s}(\Delta, -\delta, -\theta, \mathcal{M}_x \mathbf{k}). \quad (\text{S90})$$

Combining Eq. (S84) and (S90), we obtain the dependence of the spin shift vector on δ :

$$\mathbf{r}^s(\Delta, \delta, \theta, \mathbf{k}) = -\mathbf{r}^s(\Delta, -\delta, \theta, -\mathbf{k}). \quad (\text{S91})$$

We observe that the sublattice potential difference δ plays a similar role with the interlayer potential difference Δ in Eq. (S78).

II. Strained Shift Photocurrent Induced by Unpolarised Light

In this section, we show that in strained vdW materials and homostructures, the SPC induced by unpolarised light is nonzero due to broken discrete rotational symmetry. For brevity, we will omit the implicit dependence of the shift vector $\mathbf{r}(\theta, \mathbf{k})$ in stacking configuration index η , spin s , interlayer potential difference Δ and sublattice potential difference δ in this section.

The strained SPC induced by unpolarised light can be calculated by integrating $\mathbf{j}(\theta)$ all distinct polarisation angles:

$$\mathbf{J}^{\text{tot}} = \int_{-\pi/2}^{\pi/2} \mathbf{j}(\theta) d\theta = C \int_{-\pi/2}^{\pi/2} d\theta \int d\mathbf{k} \rho(\mathbf{k}) |\nu_\theta(\mathbf{k})|^2 \mathbf{r}(\theta, \mathbf{k}). \quad (\text{S92})$$

We can write $|\nu_\theta(\mathbf{k})|^2 = V_s(\theta, \mathbf{k}) + V_a(\theta, \mathbf{k})$, where $V_s(\theta, \mathbf{k}) = |\nu_x(\mathbf{k})|^2 \cos^2 \theta + |\nu_y(\mathbf{k})|^2 \sin^2 \theta$ is the component symmetric with respect to $\theta \rightarrow -\theta$, and $V_a(\theta, \mathbf{k}) = 2\text{Re} [\nu_x(\mathbf{k}) \nu_y^*(\mathbf{k})] \sin \theta \cos \theta$ is the component antisymmetric with respect to $\theta \rightarrow -\theta$. Also, we note that $\rho(\mathbf{k})$ is only dependent on the dispersion and is thus symmetric in θ . Then the integration in Eq. (S92) can be rewritten as

$$\mathbf{J}^{\text{tot}} = C \int_0^{\pi/2} d\theta \int d\mathbf{k} \rho(\mathbf{k}) [V_s(\theta, \mathbf{k}) (\mathbf{r}(\theta, \mathbf{k}) + \mathbf{r}(-\theta, \mathbf{k})) + V_a(\theta, \mathbf{k}) (\mathbf{r}(\theta, \mathbf{k}) - \mathbf{r}(-\theta, \mathbf{k}))]. \quad (\text{S93})$$

When strain is applied either parallel or perpendicular to a mirror axis, mirror symmetry about the mirror axis is preserved. For instance, when strain is applied perpendicular or parallel to y in any of the vdW systems discussed above (Bernal stacked BLG, G/hBN, monolayer TMD and 2H stacked bilayer TMD), time reversal symmetry \mathcal{T} and mirror symmetry \mathcal{M}_y are preserved. As we now show, this symmetry dramatically constrain the integrand of Eq. (S93).

To see this, we examine J_x^{tot} and J_y^{tot} separately. We first concentrate on J_x^{tot} . We note that mirror symmetry y [in particular, the first equation in Eq. (S23)] guarantees that $r_x(\theta, \mathbf{k}) + r_x(-\theta, \mathbf{k})$ is odd in k_y while $V_s(\theta, \mathbf{k})$ is even in k -space. Thus the term proportional to $V_s(\theta, \mathbf{k})$ in the integration in Eq. (S93) vanishes. Furthermore, $r_x(\theta, \mathbf{k}) - r_x(-\theta, \mathbf{k})$ is even in k_y while $V_a(\theta, \mathbf{k})$ is odd [since $\nu_y(\mathbf{k})$ is odd while $\nu_x(\mathbf{k})$ is even]. Thus the term proportional to $V_a(\theta, \mathbf{k})$ also vanishes after integration. Therefore, $J_x^{\text{tot}} = 0$ in the presence of \mathcal{T} and \mathcal{M}_y .

We now employ a similar argument for J_y^{tot} . We note that that mirror symmetry about y [in particular, the second equation in Eq. (S23)] guarantees that $r_y(\theta, \mathbf{k}) + r_y(-\theta, \mathbf{k})$ is even in k_y so that the term proportional to $V_s(\theta, \mathbf{k})$ is even. Furthermore, $r_y(\theta, \mathbf{k}) - r_y(-\theta, \mathbf{k})$ is odd in k_y so that the term proportional to $V_a(\theta, \mathbf{k})$ is also even in k_y . Thus J_y^{tot} is finite and the SPC induced by unpolarised light is directed along the y axis. As a result, when strain is applied either perpendicular or parallel to a mirror axis, \mathbf{J}^{tot} is directed along the mirror axis, as discussed in the main text. However, when strain is not applied either perpendicular or parallel to a mirror axis, \mathbf{J}^{tot} does not generically point in a symmetry determined direction; instead its direction is determined by the details of the strain, as discussed in the main text.

Importantly, this argument (presented above) for the integrated SPC over all polarizations (i.e. SPC for unpolarized light) applies for in the presence of any (and multiple) mirror planes. For instance, in the absence of strain, the vdW materials and homostructures discussed above possess an in-plane rotational symmetry C_3^z . This means that vdW materials discussed above possess multiple non-parallel mirror planes. Upon irradiation of unpolarised light and in an unstrained system, it is impossible for \mathbf{J}^{tot} to be directed along all these non-parallel reflection axes simultaneously, and thus the integrated SPC has to vanish.

III. Hamiltonian of Bernal Stacked BLG

In this section, we derive the low-energy four-band Hamiltonian for Bernal stacked BLG from the tight-binding model. Bernal stacked BLG (Fig. 1c in the main text) has a triangular lattice with primitive lattice vectors given by

$$\mathbf{a}_1 = \left(\frac{a}{2}, \frac{\sqrt{3}a}{2} \right), \quad \mathbf{a}_2 = \left(\frac{a}{2}, -\frac{\sqrt{3}a}{2} \right), \quad (\text{S94})$$

where $a = 0.246$ nm. Each unit cell contains four atoms, two from the top layer (A_t, B_t) and two from the bottom layer (A_b and B_b). In AB stacking configuration, the sublattice site of the top layer A_t is directly on top of the sublattice site B_b of the bottom layer (referred to as the dimer site), while site B_t sits at the centre of the honeycomb lattice of the bottom layer (referred to as the non-dimer site). In BA stacking, we have B_t directly on top of A_b instead. As we remarked in the previous section, these two stacking configurations are obtained by flipping one about the in-plane axis and they have the same dispersion relations.

Now we derive the four band tight-binding Hamiltonian of the system $H^{(\eta)}$ in the basis $\{\psi_{A_b}, \psi_{B_b}, \psi_{A_t}, \psi_{B_t}\}$. When an interlayer electric potential difference is applied, the top and bottom lattice sites acquire different onsite energies leading to nonzero on-diagonal terms in the tight-binding Hamiltonian: $H_{A_b A_b}^{(\eta)} = H_{B_b B_b}^{(\eta)} = \Delta/2$ and $H_{A_t A_t}^{(\eta)} = H_{B_t B_t}^{(\eta)} = -\Delta/2$.

Furthermore, the intralayer nearest-neighbour hopping from site A to site B is described the vectors

$$\boldsymbol{\delta}_1 = \left(0, \frac{a}{\sqrt{3}}\right), \quad \boldsymbol{\delta}_2 = \left(\frac{a}{2}, -\frac{a}{2\sqrt{3}}\right), \quad \boldsymbol{\delta}_3 = \left(-\frac{a}{2}, -\frac{a}{2\sqrt{3}}\right). \quad (\text{S95})$$

Thus, the intralayer hopping in each layer is described by $H_{A_b B_b}^{(\eta)} = H_{A_t B_t}^{(\eta)} = -\gamma_0 f(\mathbf{k})$, where $\gamma_0 \approx 3$ eV is the nearest neighbour hopping constant and

$$\begin{aligned} f(\mathbf{k}) &= \sum_{l=1}^3 e^{i\mathbf{k}\cdot\boldsymbol{\delta}_l} = e^{i\frac{a}{\sqrt{3}}k_y} + e^{i(\frac{a}{2}k_x - \frac{a}{2\sqrt{3}}k_y)} + e^{i(-\frac{a}{2}k_x - \frac{a}{2\sqrt{3}}k_y)} \\ &= e^{i\frac{a}{\sqrt{3}}k_y} + 2e^{-i\frac{a}{2\sqrt{3}}k_y} \cos\left(\frac{a}{2}k_x\right). \end{aligned} \quad (\text{S96})$$

In AB stacking, since A_t is directly on top of B_b , the interlayer coupling at the dimer site is given by $H_{A_t B_b}^{(\text{AB})} = H_{B_b A_t}^{(\text{AB})} = \gamma_1$. The skew interlayer hopping from A_b to B_t at the non-dimer sites involves in-plane hopping described by the in-plane vectors $-\boldsymbol{\delta}_1$, $-\boldsymbol{\delta}_2$ and $-\boldsymbol{\delta}_3$, thus the skew interlayer coupling is given by $H_{A_b B_t}^{(\text{AB})} = -\gamma_3 \sum_{l=1}^3 e^{i\mathbf{k}\cdot(-\boldsymbol{\delta}_l)} = -\gamma_3 f^*(\mathbf{k})$. The next next nearest neighbour interlayer hopping between A_b and A_t as well as between B_b and B_t is much smaller than the other terms and can be neglected here. Therefore, we arrive at the tight-binding Hamiltonian for the AB stacked BLG:

$$H^{(\text{AB})}(\mathbf{k}) = \begin{pmatrix} \frac{\Delta}{2} & -\gamma_0 f(\mathbf{k}) & 0 & -\gamma_3 f^*(\mathbf{k}) \\ -\gamma_0 f^*(\mathbf{k}) & \frac{\Delta}{2} & \gamma_1 & 0 \\ 0 & \gamma_1 & -\frac{\Delta}{2} & -\gamma_0 f(\mathbf{k}) \\ -\gamma_3 f(\mathbf{k}) & 0 & -\gamma_0 f^*(\mathbf{k}) & -\frac{\Delta}{2} \end{pmatrix} \quad (\text{S97})$$

In BA stacking, B_t is directly on top of A_b , and the interlayer coupling at the dimer site is $H_{B_t A_b}^{(\text{BA})} = H_{A_b B_t}^{(\text{BA})} = \gamma_1$. The skew interlayer hopping from B_b to A_t is given by the in-plane vectors $\boldsymbol{\delta}_1$, $\boldsymbol{\delta}_2$ and $\boldsymbol{\delta}_3$, yielding $H_{B_b A_t}^{(\text{BA})} = -\gamma_3 f(\mathbf{k})$. Thus the Hamiltonian for the BA stacked BLG is

$$H^{(\text{BA})}(\mathbf{k}) = \begin{pmatrix} \frac{\Delta}{2} & -\gamma_0 f(\mathbf{k}) & 0 & \gamma_1 \\ -\gamma_0 f^*(\mathbf{k}) & \frac{\Delta}{2} & -\gamma_3 f(\mathbf{k}) & 0 \\ 0 & -\gamma_3 f^*(\mathbf{k}) & -\frac{\Delta}{2} & -\gamma_0 f(\mathbf{k}) \\ \gamma_1 & 0 & -\gamma_0 f^*(\mathbf{k}) & -\frac{\Delta}{2} \end{pmatrix}. \quad (\text{S98})$$

We note that for the Hamiltonians above, the band extrema occur at the corners of the Brillouin zone labeled by $\mathbf{K}_+ = (\frac{4\pi}{3a}, 0)$ and $\mathbf{K}_- = -\mathbf{K}_+$. At low energy, the tight-binding Hamiltonian can be approximated up to the linear order of $\mathbf{p} = \mathbf{k} - \mathbf{K}_\xi$ around each valley $\xi = \pm$. By expanding $f(\mathbf{k})$ around \mathbf{K}_ξ , we obtain

$$H^{(\text{AB})}(\mathbf{p}) = \begin{pmatrix} \frac{\Delta}{2} & \hbar v p^\dagger & 0 & \hbar v_3 p \\ \hbar v p & \frac{\Delta}{2} & \gamma_1 & 0 \\ 0 & \gamma_1 & -\frac{\Delta}{2} & \hbar v p^\dagger \\ \hbar v_3 p^\dagger & 0 & \hbar v p & -\frac{\Delta}{2} \end{pmatrix}, \quad H^{(\text{BA})}(\mathbf{p}) = \begin{pmatrix} \frac{\Delta}{2} & \hbar v p^\dagger & 0 & \gamma_1 \\ \hbar v p & \frac{\Delta}{2} & \hbar v_3 p^\dagger & 0 \\ 0 & \hbar v_3 p & -\frac{\Delta}{2} & \hbar v p^\dagger \\ \gamma_1 & 0 & \hbar v p & -\frac{\Delta}{2} \end{pmatrix}, \quad (\text{S99})$$

where $p = \xi p_x + i p_y$, $v = \sqrt{3}a\gamma_0/2\hbar$ is the Fermi velocity in each layer and $v_3 = \sqrt{3}a\gamma_3/2\hbar$.

IV. Numerical Calculation of Shift Vector in AB stacked BLG for other polarizations

Using the four-band Hamiltonian derived in the previous section, we numerically calculate the weighted shift vectors $\mathbf{R}^{(n)}(\Delta, \theta, \mathbf{p})$ in k -space in the vicinity of the Dirac point. In the main text, we have shown $\mathbf{R}^{(n)}(\Delta, \theta, \mathbf{p})$ in AB/BA stacked BLG for the x -polarised electric at the K_+ valley. Here we plot the $\mathbf{R}^{(\text{AB})}(\Delta, \theta, \mathbf{p})$ at $\theta = \pi/2$ (Fig. S1a and b) and $\theta = 2\pi/3$ (Fig. S1c and d) at K_+ and K_- valleys.

We note that for $\mathbf{K}_\pm = (\pm\frac{4\pi}{3a}, 0)$ and \mathbf{k} measured from the Γ point, $k_x \rightarrow -k_x$ maps p_x at the K_\pm valley to $-p_x$ at the K_\mp valley, while $k_y \rightarrow -k_y$ maps $p_y \rightarrow -p_y$ at the same valley. Using these identities, we observe that for the electric field polarisation along with the mirror plane (y -axis, $\theta = \pi/2$), the shift vectors in Fig. S1a and b obey the relations in Eq. (S22) and (S23). From p_x at the K_+ valley to $-p_x$ at the K_- valley, $R_x^{(\text{AB})}$ switches sign and

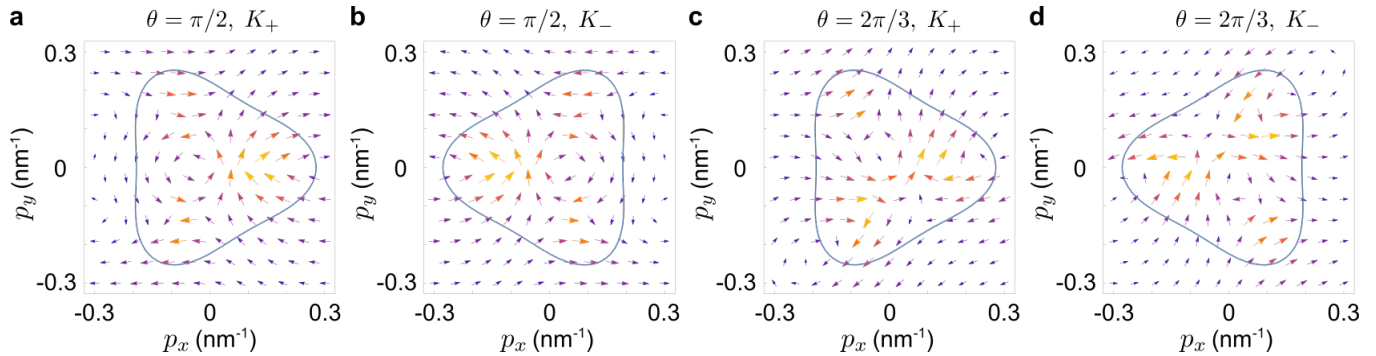


FIG. S1: (a,b) Plot of $\mathbf{R}^{(AB)}(\Delta, \theta = \pi/2, \mathbf{p})$ at the K_+ (a) and K_- (b) valley. (c,d) Plot of $\mathbf{R}^{(AB)}(\Delta, \theta = 2\pi/3, \mathbf{p})$ at the K_+ (c) and K_- (d) valley. Similar to that found in the main text, we have taken $\Delta = 20$ meV. All other parameters are the same as Fig. 2 in the main text.

$R_y^{(AB)}$ remains unchanged. For $p_y \rightarrow -p_y$ in each valley, $R_x^{(AB)}$ is also odd while $R_y^{(AB)}$ is even. This leads to a shift photocurrent flowing along the y axis.

Furthermore, when the electric field is perpendicular to one of the reflection axis ($\theta = 2\pi/3$), we observe that the weighted shift vector component normal to the polarisation is even, while the component parallel to the polarisation is odd (e.g. Fig. S1c and d), leading to a transverse shift photocurrent.

-
- (1) Sipe, J. E.; Shkrebtii, A. I. Second-order optical response in semiconductors. *Phys. Rev. B* **2000**, *61*, 5337-5352.
 - (2) Morimoto, T.; Nagaoso, N. Topological nature of nonlinear optical effects in solids. *Sci. Adv.* **2016**, *2*, e1501524.
 - (3) Shi, L-K.; Song, J. C. W. Shift vector as the geometric origin of beam shifts. *Phys. Rev. B* **2019**, *100*, 201405(R).
 - (4) Shi, L-K.; Zhang, D.; Chang, K.; Song, J. C. W. Geometric photon-drag effect and nonlinear shift current in centrosymmetric crystals. 2020 (available at <https://arxiv.org/abs/2006.08358>).